American Journal of Pathology, Vol. 153, No. 4, October 1998

Angiogenesis in Mice with Chronic Airway Inflammation

Strain-Dependent Differences

Gavin Thurston,* Thomas J. Murphy,* Peter Baluk,* J. Russell Lindsey,† and Donald M. McDonald*

From the Department of Anatomy and Cardiovascular Research Institute, University of California, San Francisco, California, and the Department of Comparative Medicine,† University of Alabama, Birmingham, Alabama*

Chronic inflammation is associated with blood vessel proliferation and enlargement and changes in vessel phenotype. We sought to determine whether these changes represent different types of angiogenesis and whether they are stimulus dependent. Chronic airway inflammation, produced by infection with *Mycoplasma pulmonis*, was compared in strains of mice known to be resistant (C57BL/6) or susceptible (C3H). Tracheal vascularity, assessed in whole mounts after *Lycopersicon esculentum* lectin staining, increased in both strains at 1, 2, 4, and 8 weeks after infection, but the type of vascular remodeling was different. The number of vessels doubled in tracheas of C57BL/6 mice, with corresponding increases of capillaries and venules. In contrast, neither the number nor the length of vessels changed in C3H mice. Instead, vessel diameter and endothelial cell number doubled, and the proportion of venules doubled with a corresponding decrease of capillaries. Although the infection had no effect on baseline plasma leakage, in both strains it potentiated the leakage produced by substance P. We conclude that the same stimulus can result in blood vessel proliferation or enlargement, depending on the host response. Endothelial cells proliferate in both cases, but in one case new capillaries form whereas in the other capillaries convert to venules. *(Am J Pathol 1998, 153:1099–1112)*

Angiogenesis, characterized by the growth of new vessels from existing ones,[1] occurs in many inflammatory diseases. In rheumatoid arthritis, for example, new vessels invade the normally avascular synovium.[2–4] However, angiogenesis is not the only change in the microvasculature that occurs in chronic inflammation. Under some pathological conditions, microvessels may enlarge, lengthen, or become tortuous, without the growth of new vessels. The enlarged vessels may contain proliferating endothelial cells. Enlarged, congested blood vessels are a well documented feature of asthma[5–7] and psoriasis.[8–14]

Chronic inflammation may also be accompanied by changes in the phenotype of endothelial cells.[11] In the chronic airway disease produced in rats by *Mycoplasma pulmonis* infection, for example, substance P induces plasma leakage not only from venules but also from newly formed capillary-like vessels.[15] In comparison, in the airway mucosa of normal rats, substance P causes plasma leakage from venules but not capillaries.[16] The leakage from capillary-like vessels in infected rats is due to a change in the phenotype of capillary endothelial cells, one feature of which is increased expression of neurokinin receptors.[15]

It is unclear whether new vessel growth and vessel enlargement are distinct processes, different stages of a single process, or processes typical of particular tissues or particular inflammatory stimuli. Furthermore, it is unclear whether changes of endothelial cell phenotype are a consistent feature of chronic inflammation.

We have sought to examine these issues by developing an animal model to study the stages and types of microvascular remodeling associated with chronic airway inflammation. For this purpose we have used *M. pulmonis* infection of the respiratory tract of rats and mice. Our previous studies have shown that the growth of new blood vessels is a prominent feature of the chronically inflamed airway mucosa of infected rats.[15,17] Although less is known about vascular remodeling in the airways of infected mice, studies have shown that the severity of *M. pulmonis*-induced respiratory disease in mice is strain dependent.[18–20] Such studies can take advantage of the wealth of information on immune and inflammatory responses in mice and the advent of genetically targeted mutants, which could eventually be used to address molecular mechanisms of vascular remodeling.

The overall goal of the present study was to develop a better understanding of the distinction between new ves-

Supported in part by NIH grants HL-24136 and HL-59157.

Accepted for publication July 18, 1998.

Address reprint requests to Dr. Gavin Thurston, Department of Anatomy, Box 0452, 505 Parnassus, Rm. 850-HSW, University of California, San Francisco, CA 94143-0452. E-mail: gavint@itsa.ucsf.edu.

sel growth and vessel enlargement in a model of chronic inflammation in mice. In particular, we sought to compare the stages of vascular remodeling in mouse strains with known differences in severity of respiratory disease after infection with *M. pulmonis*. We used C57BL/6 mice, which develop mild disease, and C3H mice, which develop severe disease.[18–20] Previous studies have shown that, compared with C57BL/6 mice, C3H mice have greater airway exudate, epithelial hyperplasia, lymphoid hyperplasia, and inflammatory cell infiltrate in the alveoli and have higher mortality.[18]

Our specific aims were to 1) determine whether the vascular remodeling in C57BL/6 and C3H mice infected with *M. pulmonis* involves the growth of new blood vessels, changes in existing vessels, or both, 2) determine whether the enlargement of vessels after infection is accompanied by an increase in number or size of endothelial cells, 3) characterize changes in endothelial cell phenotype associated with vascular remodeling in chronic airway disease, and 4) determine whether the remodeled vessels are abnormally leaky under baseline conditions or are abnormally sensitive to inflammatory mediators.

Our strategy was to induce *M. pulmonis* infection in pathogen-free C57BL/6 and C3H mice by intranasal inoculation. At 1, 2, 4, or 8 weeks after inoculation the tracheal microvasculature was stained by perfusion of the lectin *Lycopersicon esculentum*,[21] and the number, size, and length of vessels were measured morphometrically. Alternatively, endothelial cell borders were stained by vascular perfusion of silver nitrate,[16] and the number and size of endothelial cells were measured. The phenotype of the endothelial cells was characterized by the binding of lectins,[21] expression of von Willebrand factor (vWF),[22] and adhesion of leukocytes. In all cases, the three-dimensional architecture of the vessels was analyzed in tracheal whole mounts. In addition, endothelial permeability was assessed *in vivo* under baseline conditions and after substance P, by measuring the leakage of intravascular Evans blue dye.[23]

Materials and Methods

Infection of Mice with Mycoplasma pulmonis

Pathogen-free, 8-week-old, male and female C3H mice (Frederick Cancer Research Facility, Frederick, MD (C3H/HeNCr) or Charles River Laboratories, Hollister, CA (C3H/HeNCrlBR)) and C57BL/6 mice (Charles River (C57BL/6NCrlBR)) were used in these experiments. Mice were anesthetized (87 mg/kg ketamine and 13 mg/kg xylazine intraperitoneally) and inoculated intranasally with $\sim 10^5$ colony-forming units of *M. pulmonis* (strain UAB CT_7) in a volume of 50 μl. Infected and pathogen-free control mice were caged and housed separately under barrier conditions and handled in accordance with the procedures of the Committee on Animal Research, University of California, San Francisco.

Vascular Perfusions and Staining

At 1, 2, 4, or 8 weeks after inoculation, mice were anesthetized with Nembutal (30 to 50 mg/kg intraperitoneally) and supplemented as necessary. Infected mice tended to be more sensitive to anesthetic and were given less for the initial injection. Titers of antibody to *M. pulmonis* were measured in serum from pathogen-free control and infected mice at the time of the experiment. Blood (0.2 ml) was withdrawn from the jugular vein into a heparinized syringe and centrifuged for 6 minutes at 8000 rpm. Plasma was withdrawn and re-centrifuged, and 100 μl of the plasma was added to 400 μl of sterile saline, heated to 56°C for 30 minutes, and then frozen until sent for analysis (MA Bioservices, Rockville, MD).

To perfuse the mice, the chest cavity was opened, the atria were removed to allow outflow of blood and perfusate, and a cut was made in the left ventricle. A cannula was inserted into the ascending aorta and clamped. Fixative or other solutions were perfused at 120 mm Hg. The luminal surface of the vasculature of some mice was stained by perfusion of biotinylated *L. esculentum* lectin[21] (Vector Laboratories, Burlingame, CA). The vasculature was perfusion fixed for 3 minutes with 1% paraformaldehyde and 0.5% glutaraldehyde in phosphate-buffered saline (PBS), pH 7.4, and the vasculature was then perfused with PBS for 60 seconds, 25 ml of PBS plus 1% bovine serum albumin (BSA) for 80 seconds, 25 ml of lectin (5 or 10 μg/ml in PBS/BSA) for 80 seconds, 25 ml of PBS/BSA for 60 seconds, and PBS for 60 seconds. The tracheas were removed, opened flat, and stained using avidin-biotin complex/diaminobenzidine (ABC/DAB) histochemistry.[21] Tracheas were dehydrated through alcohols and mounted whole in Permount embedding medium. The rostral portions of some tracheas were embedded in glycol methacrylate, sectioned (3 to 4 μm thickness), stained with toluidine blue, and mounted in Permount embedding medium.

The endothelial cell borders were stained in the vasculature of some mice by perfusion of silver nitrate.[16] The vasculature was perfusion fixed for 3 minutes with 1% paraformaldehyde and 0.5% glutaraldehyde in 75 mmol/L cacodylate, pH 7.4, and the the vasculature was then perfused with 0.9% NaCl for 1 minute, 10 ml of 5% glucose for 10 seconds, 7 ml of 0.2% silver nitrate for 7 seconds, 10 ml of 5% glucose for 10 seconds, and fixative for 60 seconds. The tracheas were removed and opened flat, exposed to light for 15 minutes to develop the silver, and then dehydrated through alcohols and mounted whole in Permount. Tracheas stained with biotinylated lectins or silver nitrate were examined with an upright microscope (Axiophot, Zeiss) equipped with Nomarski differential interference contrast optics.

Morphometric Measurements of Vessels and Endothelial Cells

Morphometric measurements of blood vessels were made in whole mounts of tracheas stained with lectin or silver nitrate using a Zeiss Axiophot microscope coupled

to a color charge-coupled device (CCD) video camera (Sony, model DXC-750), a digitizing card (VideoLogic DVA-4000, Cambridge, MA), monitor, and software written for this purpose in our laboratory.[16] Vessel area density, which represents the fraction of the total tissue area occupied by the wall or lumen and reflects the overall number, length, and size of vessels, was measured in lectin-stained tracheas by overlaying the live video microscopic image with a computer-generated square lattice. The number of points of the lattice that intersected vessels was scored. Vessel area density was expressed as the fraction (percentage) of lattice points that intersected vessels. Vessel length density, which represents the length of blood vessels in a given area of tissue and reflects the total length of vessels independent of vessel size and number, was measured by overlaying an array of sinusoidal lines, and the number of intersections of vessels with the lines was scored. Length density was computed from the total line length and number of intersections. Measurements of vessel area density and vessel length density were made on 10 fields per trachea and four tracheas per group ($n = 4$). The diameter of different types of tracheal microvessels was measured in 10 vessels of each type per trachea and four tracheas per group ($n = 4$). We used the number of vessels that traverse the cartilage as an index of the number of vessels in the trachea. This index was determined by placing a line of known length on the video screen parallel to the axis of the cartilage and counting the number of vessels that intersected the line. Results were expressed as the number of vessels per unit length of the intersection line (number per millimeter). Measurements were made on 10 cartilage segments per trachea and four tracheas per group ($n = 4$). Luminal endothelial cell surface area was measured in silver-stained venules by tracing the cell border of 10 endothelial cells per trachea and four tracheas per group ($n = 4$).

Characterization of Endothelial Cell Phenotype

Binding of Wheat Germ Agglutinin Lectin

Previous studies in the airways of rats have shown that the luminal surface of endothelial cells in venules does not bind the lectin wheat germ agglutinin (WGA), whereas that of endothelial cells in arterioles and capillaries does.[21] The vessels in the airways of mice bind WGA in a similar pattern; thus, the pattern of WGA binding was used as one feature of the phenotype of the endothelial cells in remodeled vessels of infected mice. Biotinylated WGA (Vector) was perfused through the vasculature of pathogen-free and infected C57BL/6 and C3H mice, and the tracheas were processed using a protocol similar to that used with *L. esculentum* lectin (see above).

Staining for von Willebrand Factor

Previous studies have shown that vWF immunoreactivity is greater on the venous side of the circulation.[22,24–26] We characterized the distribution of vWF in tracheal whole mounts in which the vessels were stained by perfusion of fluorescein-*L. esculentum* lectin. vWF was stained by immersing the intact trachea in antibodies to vWF. The vasculature was perfusion fixed for 3 minutes with 1% paraformaldehyde in PBS, pH 7.4, and then perfused with PBS for 60 seconds, 25 ml of PBS plus 1% BSA for 80 seconds, 25 ml of fluorescein *L. esculentum* lectin (20 μg/ml in PBS/BSA) for 80 seconds, 25 ml of PBS/BSA for 60 seconds, and PBS for 60 seconds. The tracheas were removed, opened flat, and pinned on slabs of Sylgard (Dow Corning, Midland, MI). The tracheas were permeabilized in PBS plus 0.3% Triton X-100 (Sigma Chemical Co., St. Louis, MO) for 3 hours, incubated overnight with rabbit polyclonal primary antibody to vWF (diluted 1:400; Dako, Carpinteria, CA), washed, incubated for 4 to 6 hours with Cy3-conjugated goat anti-rabbit secondary antibody (diluted 1:200; Jackson ImmunoResearch Laboratories, West Grove, PA), washed, and mounted intact in Vectashield (Vector). Fluorescently stained tracheas were examined with a confocal microscope (Zeiss LSM 410).

Adhesion of Leukocytes

Adherent leukocytes were readily visible in tracheal vessels perfused with biotinylated *L. esculentum* lectin and stained by the ABC/DAB peroxidase reaction (see above). Using video microscopy (see above), the number of adherent leukocytes was determined in segments of vessels in the position of capillaries overlying the tracheal cartilage. The length and diameter of each vessel segment were also measured, and the number of leukocytes expressed as the number per luminal vessel surface area. Measurements were made on 10 vessels per trachea and four tracheas per group ($n = 4$).

Measurement of Relative Abundance of Segments of the Microvasculature

The abundance of arterioles, capillaries, and venules was determined morphometrically in *L. esculentum*-stained tracheal whole mounts. Using video projections and a digitizing tablet as described above, the length of each type of microvessel segment was traced in an entire video microscopic field. The tracheal vasculature in mice was organized in a pattern similar to that in rats,[16] although there were fewer branches between feeding arterioles and collecting venules. The microscope fields measured approximately 360 $\times$ 580 μm. The length of blood vessels per unit area of tracheal tissue (vessel length density, mm/mm^2) and the fraction (percentage) of the total vessel length were calculated for each type of microvessel in each of four microscope fields per trachea and four tracheas per group ($n = 4$).

Measurement of Plasma Leakage

The amount of plasma leakage was compared in the tracheas of pathogen-free mice and mice infected with *M. pulmonis* for 4 weeks. Leakage was measured in the

baseline state and after intravenous injection of the inflammatory mediator substance P. Plasma leakage was measured using the tracer dye Evans blue as described previously.[23] Briefly, Evans blue (30 mg/kg; EM Sciences, Cherry Hill, NJ) was injected into one femoral vein of anesthetized mice, and 30 seconds later substance P (5 μg/kg in 100 μl) or vehicle was injected into the other femoral vein. Five minutes later the vasculature was perfusion fixed (1% paraformaldehyde in 50 mmol/L citrate buffer, pH 3.5) for 1 minute. Tracheas were removed, blotted dry, and weighed. Evans blue was extracted from the tracheas with formamide and measured with a spectrophotometer. Measurements were made in eight vehicle-treated (baseline) mice ($n = 8$) and six substance-P-stimulated mice ($n = 6$).

Statistics

Data are presented as means ± SE of data from four tracheas per group except where otherwise noted. Significant differences between means were evaluated using analysis of variance followed by Dunn-Bonferroni's test or unpaired Student's *t*-test. $P < 0.05$ was considered statistically significant.

Results

Comparison of Vascular Remodeling in C57BL/6 and C3H Mice

The architecture of the tracheal vessels in pathogen-free C57BL/6 mice and C3H mice resembled that in pathogen-free rats.[16] The vessels in lectin-stained tracheal whole mounts formed repeating, orderly networks: feeding arterioles were in most of the intercartilaginous regions parallel to the cartilaginous rings, terminal arterioles branched from the feeding arterioles toward the cartilaginous rings, capillaries crossed the cartilaginous rings, postcapillary venules were near the edge of the rings, and collecting venules were in the intercartilaginous region parallel to the rings (Figure 1, A and E). Most of the vessels were in a plane of the mucosa beneath the epithelial basement membrane.

After infection with *M. pulmonis*, the tracheal microvasculature was conspicuously abnormal in both strains of mice, but the abnormality differed in the two strains. The tracheal vessels in C57BL/6 mice were enlarged at 1 and 2 weeks after infection (Figure 1B), were enlarged and slightly increased in number at 4 weeks (Figure 1C), and were much more numerous at 8 weeks (Figure 1D). This new vessel network was no longer confined to a single plane, and some vessels were perpendicular to the epithelium (Figure 1D). The venules were enlarged at all time points (Figure 1, B–D). Vascularity of the tracheal mucosa of C57BL/6 mice, as measured by the area density of vessels, increased from a pathogen-free baseline value of 34% to 49% at 1 week after infection to 64% at 8 weeks (Figure 2A). The total length of tracheal vessels in C57BL/6 mice, estimated by length density measurements, was 40% higher than baseline at 8 weeks after infection (Figure 3A), and the number of vessels crossing each cartilaginous ring was 120% higher than baseline at 8 weeks (Figure 3B).

In comparison, the tracheal vessels in C3H mice infected with *M. pulmonis* were enlarged at 1 and 2 weeks after infection and remained enlarged at 4 and 8 weeks without an increase in the number of vessels (Figure 1, E and F). The vessel area density in tracheas of C3H mice increased from a baseline value of 41% in pathogen-free mice to 65% at 1 week after infection and further to 64% at 8 weeks (Figure 2B). The vessel length density did not change in C3H mice (Figure 3A) nor did the number of vessels (Figure 3B). The remodeled vessels in the infected tracheas of C3H mice remained in a plane beneath the epithelium.

When viewed in tissue sections, tracheal vessels in pathogen-free mice were found in the loose connective tissue of the mucosa, and the endothelial cells were flattened (Figure 4A). In comparison, tracheal vessels in infected C57BL/6 (Figure 4B) and C3H (Figure 4C) mice were conspicuously larger in diameter and the endothelium remained flattened. The mucosa of infected mice contained numerous inflammatory cells.

These results indicate that the number of blood vessels increased in C57BL/6 mice but not in C3H mice after infection with *M. pulmonis* and that some vessels enlarged in both strains.

Increased Number of Endothelial Cells in Enlarged Vessels

Because of the conspicuous vessel enlargement in the tracheas of *M. pulmonis*-infected C3H mice, we determined whether there was an increase in the number of endothelial cells. To do so, we measured the luminal vessel surface area and the area of endothelial cells in pathogen-free and infected C3H mice. The vessel diameters in all segments of the tracheal microvasculature at 1 week and 4 weeks after infection were increased compared with pathogen-free controls (Figure 5). At 4 weeks after infection, the arteriole diameters were 1.9-fold that of pathogen-free mice, the capillaries 2.6-fold, the postcapillary venules 2.3-fold, and the collecting venules 1.7-fold.

Figure 1. Tracheal vasculature in pathogen-free and *M. pulmonis*-infected C57BL/6 and C3H mice. The vasculature was perfusion stained with biotinylated *L. esculentum* lectin and ABC/DAB peroxidase reaction and visualized by light microscopy in tracheal whole mounts. A: Organized pattern of mucosal vessels in trachea of pathogen-free C57BL/6 mouse, showing capillaries across a cartilaginous ring (cartilage), fed from arterioles (arrows) and drained by venules (arrowheads) in intercartilaginous regions (intercartilage). B: Enlarged vessels in trachea of C57BL/6 mouse at 2 weeks after infection C: Enlarged vessels and regions with increased numbers of capillary-sized vessels (arrow) in trachea of C57BL/6 mouse at 4 weeks after infection. D: Numerous capillary-sized vessels and enlarged vessels in trachea of C57BL/6 mouse at 8 weeks after infection. Many capillary-sized vessels are out of focus as vessels are no longer confined to plane of epithelium. E: Trachea of pathogen-free C3H mouse, showing organized pattern of mucosal vessels. F: Enlarged vessels in trachea of C3H mouse at 8 weeks after infection. All segments of the vasculature appear enlarged. Similar enlarged vessels were seen at 1, 2, and 4 weeks after inoculation of C3H mice. Scale bar (A–F), 100 μm.

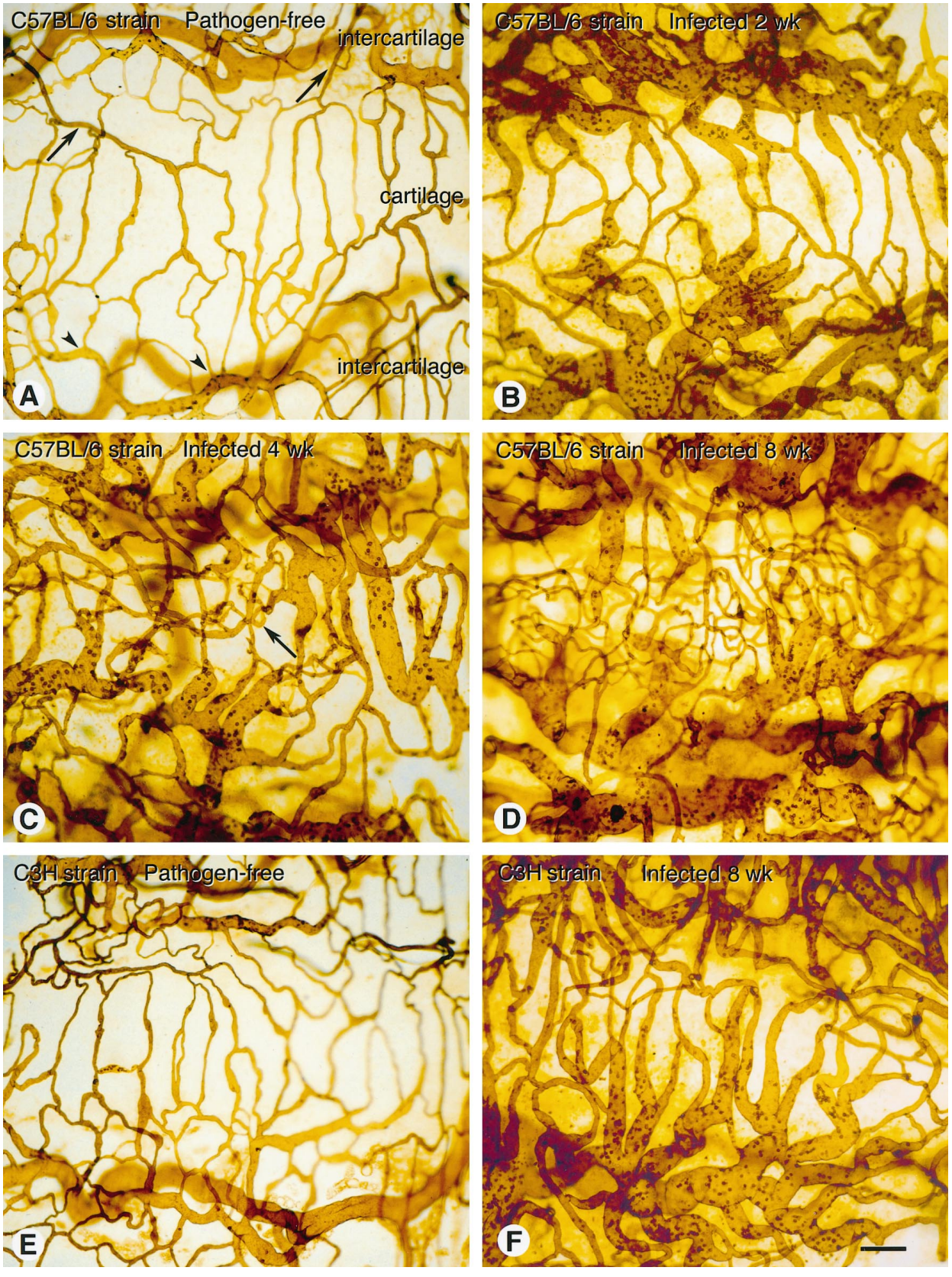
C57BL/6 strain Pathogen-free
intercartilage
cartilage
intercartilage
A
C57BL/6 strain Infected 2 wk
B
C57BL/6 strain Infected 4 wk
C
C57BL/6 strain Infected 8 wk
D
C3H strain Pathogen-free
E
C3H strain Infected 8 wk
F

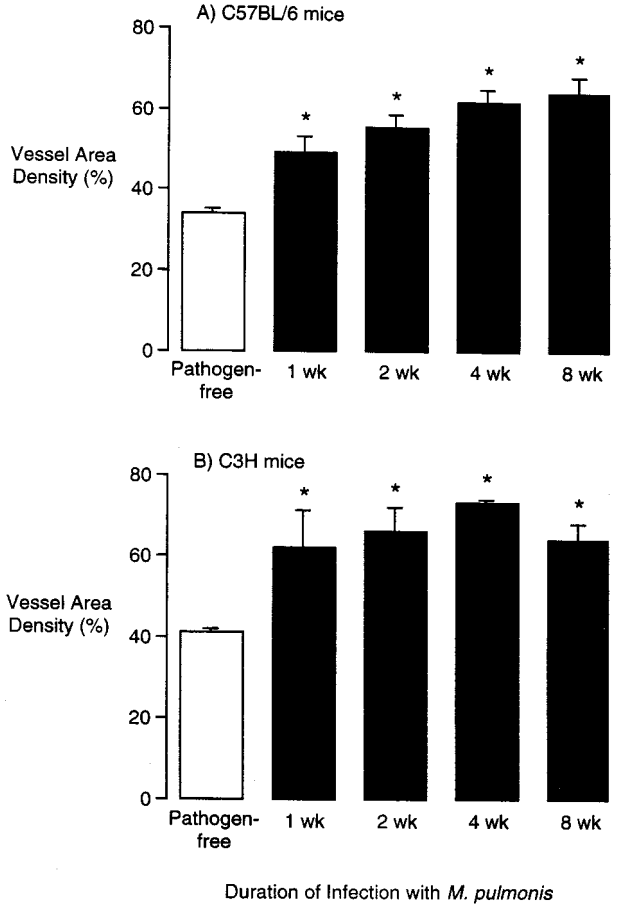

Figure 2. Vessel area density in tracheal mucosa of pathogen-free and *M. pulmonis*-infected C57BL/6 (A) and C3H (B) mice. Vessel area density was measured by morphometric point counting in *L. esculentum* lectin-stained tracheal whole mounts. Values represent mean ± SE of 6 to 10 microscope fields per trachea and four tracheas per group ($n = 4$). *Significantly different from corresponding pathogen-free value.

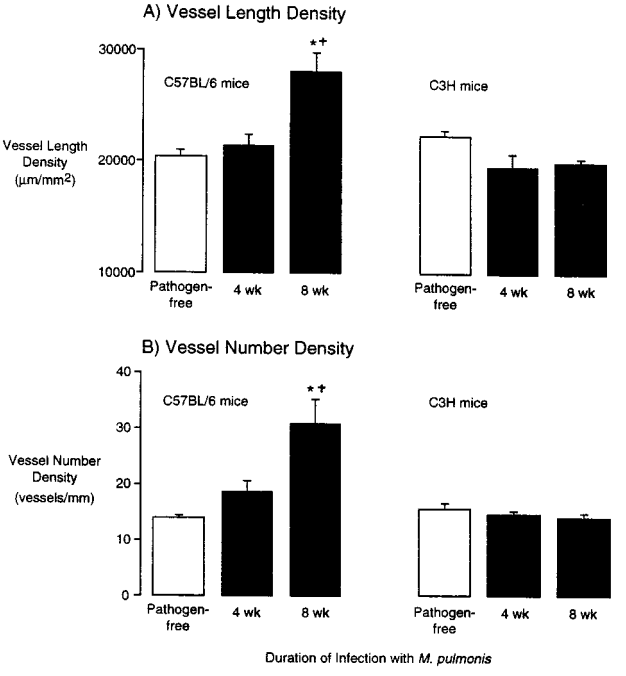

Figure 3. Vessel length density (A) and number of vessels (B) in tracheal mucosa of pathogen-free and *M. pulmonis*-infected C57BL/6 and C3H mice. Vessel length density and number of vessels were measured morphometrically in *L. esculentum* lectin-stained tracheal whole mounts. Values represent mean ± SE of 6 to 10 microscope fields per trachea and four tracheas per group ($n = 4$). *Significantly different from corresponding pathogen-free value; †significantly different from corresponding value in C3H mice.

Based on measurements of vessel length and diameter (Figure 5), the surface area of the microvasculature in infected C3H mice was 2.1-fold that of pathogen-free controls.

The average luminal surface area of endothelial cells was measured in C3H mice stained by perfusion of silver nitrate (Figure 6, A and B). Interestingly, the endothelial cell surface area was 32% greater at 1 week after infection but at 2 weeks and 4 weeks was not significantly different from the baseline values (Figure 7). Comparing the time course of the increases in vessel diameter and the changes in endothelial area suggests that the vessels were dilated at 1 week (vessel enlargement with larger endothelial cells) and then the number of endothelial cells increased at 2 and 4 weeks (vessel enlargement with normal-sized endothelial cells). However, even at 1 week, the enlargement of endothelial cells was not sufficient to account for the increased surface area of the vessels; the endothelial cells in collecting venules were 32% larger whereas the luminal surface area was 66% larger, indicating 26% more endothelial cells. At 4 weeks, the vessels remained enlarged whereas the average endothelial cell area returned to normal; thus, an estimated 71% more endothelial cells accompanied the increased surface area in collecting venules. These results indicate that the infection increased the number of endothelial cells in the tracheal vasculature of C3H mice.

Changes in Phenotype of Endothelial Cells in Remodeled Vessels

In addition to the different changes in the architecture of vessels in C57BL/6 and C3H mice after infection, some of the functional properties of the remodeled vessels were very different in the two strains. In C57BL/6 mice, new capillary-sized vessels connected to other capillary-sized vessels or to venules (Figure 6C). Numerous blind-ending vessels, which appeared to be vascular sprouts, were also present (Figure 6D). Such sprouts were common in tracheas of infected C57BL/6 mice but not in pathogen-free mice or infected C3H mice. In C3H mice, abrupt transitions in the characteristics of vessels occurred, in which arterioles joined venules with little or no intervening capillaries (Figure 6, E and F).

In addition to these changes in morphology, the remodeled vessels exhibited changes in lectin binding, vWF expression, and leukocyte adhesion.

Binding of Wheat Germ Agglutinin Lectin

One phenotypic characteristic of venular endothelial cells, unlike capillary endothelial cells, is that the lectin WGA does not bind to their luminal surface.[21] In tracheal

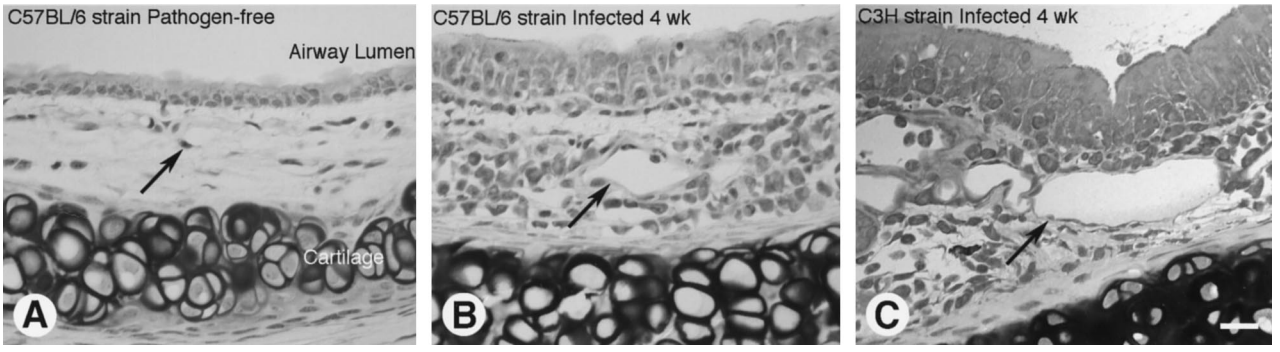

Figure 4. Histological sections of tracheas from pathogen-free and *M. pulmonis*-infected mice. Tracheas were fixed by perfusion, embedded in glycol methacrylate, sectioned, and stained with toluidine blue. A–C: Trachea from pathogen-free C57BL/6 mouse (A), 4-week-infected C57BL/6 mouse (B), and 4-week-infected C3H mouse (C). Arrows mark vessels, which are enlarged in the infected mice (B and C). Scale bar (A–C) 20 μm.

vessels of pathogen-free C3H and C57BL/6 mice, WGA bound to the luminal surface of endothelial cells in arterioles and capillaries but bound weakly or not at all in venules (Figure 8A). In C57BL/6 mice infected with *M. pulmonis*, endothelial cells in the new capillary-sized vessels bound WGA (Figure 8C), indicating a similarity to capillary endothelial cells, whereas endothelial cells in enlarged venules did not bind WGA. In infected C3H mice, endothelial cells in the enlarged vessels in the anatomical position of capillaries bound WGA weakly or not at all (Figure 8E), indicating their conversion to a venule-like phenotype.

Expression of von Willebrand Factor

vWF immunoreactivity is another marker that distinguishes endothelial cells of different segments of the vasculature.[22,24–26] In tracheal vessels of pathogen-free mice, vWF immunoreactivity was moderate in endothelial cells in arterioles, high in venules, and low in capillaries (Figure 8B). In tracheal vessels of infected C57BL/6 mice, vWF immunoreactivity was very low in endothelial cells of the new capillary-sized vessels and high in enlarged venules (Figure 8D). In infected C3H mice, vWF immunoreactivity was high in endothelial cells in the enlarged, venule-like vessels in the anatomical position of capillaries (Figure 8F).

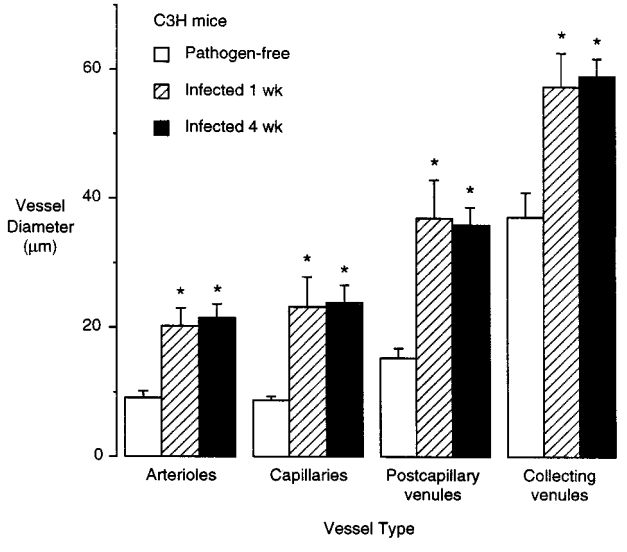

Figure 5. Vessel luminal diameter in tracheal mucosa of pathogen-free and *M. pulmonis*-infected C3H mice. Vessel diameter was measured morphometrically in *L. esculentum* lectin-stained tracheal whole mounts. Values represent mean ± SE of 10 vessels of each type per trachea and four tracheas per group ($n = 4$). *Significantly different from corresponding pathogen-free value.

Adhesion of Leukocytes

Tracheal venules in pathogen-free rats contain occasional adherent leukocytes,[27] and the number is increased by inflammatory stimuli.[16,27] Similarly, tracheal venules of pathogen-free mice contain occasional leukocytes, whereas capillaries contained almost none (Figure 1, A and E). In infected C3H mice, leukocytes were numerous in venules and in remodeled vessels in the position of capillaries (Figures 1F and 6, E and F). The number of adherent leukocytes in remodeled vessels overlaying the cartilage in the position of capillaries was more than 100-fold higher in infected C3H mice (1266 ± 100 per mm^2 of vessel surface area at 4 weeks) than in pathogen-free mice (12 ± 11 per mm^2).

Relative Proportion of Different Vessel Types

The abundance of the different types of microvessels was measured in the tracheal mucosa of C57BL/6 and C3H mice (Table 1). In C57BL/6 mice, the length density of arterioles did not change significantly at 8 weeks after infection, but the length density of capillaries increased by 73%, and the length density of venules increased by 175% compared with pathogen-free mice (Table 1). As a result, the proportion of arterioles decreased in infected C57BL/6 mice, the proportion of capillaries did not change, and the proportion of venules increased from 18% to 28%.

In C3H mice, the length density of arterioles decreased by 30% at 8 weeks after infection, the length density of capillaries decreased by 55%, and the length density of venules increased by 80% (Table 1). As a result, the proportion of venules increased from 26% in pathogen-free C3H mice to 55% in infected mice, whereas the proportion of capillaries declined from 57% to 31%.

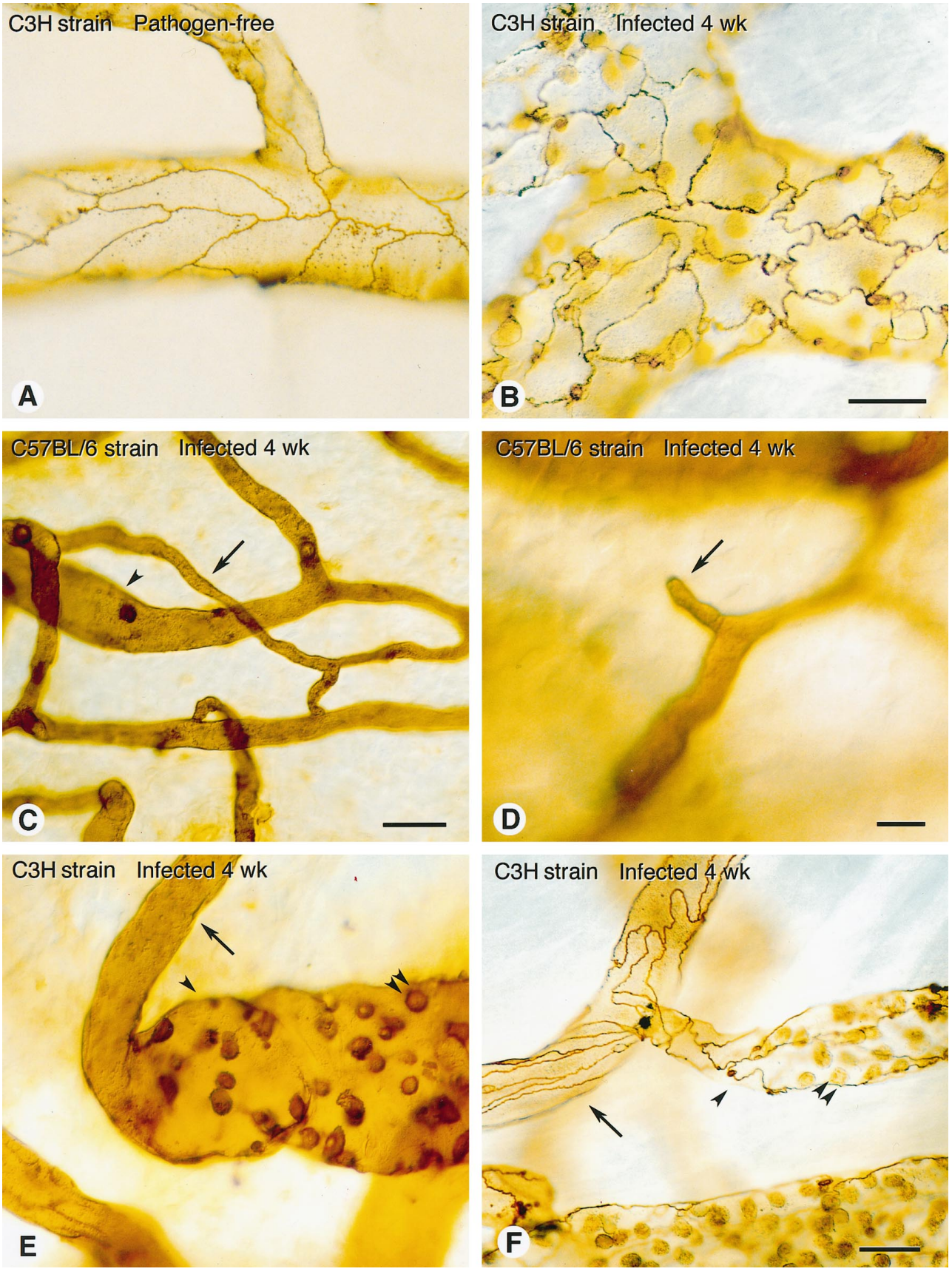
C3H strain Pathogen-free
A
C3H strain Infected 4 wk
B
C57BL/6 strain Infected 4 wk
C
C57BL/6 strain Infected 4 wk
D
C3H strain Infected 4 wk
E
C3H strain Infected 4 wk
F

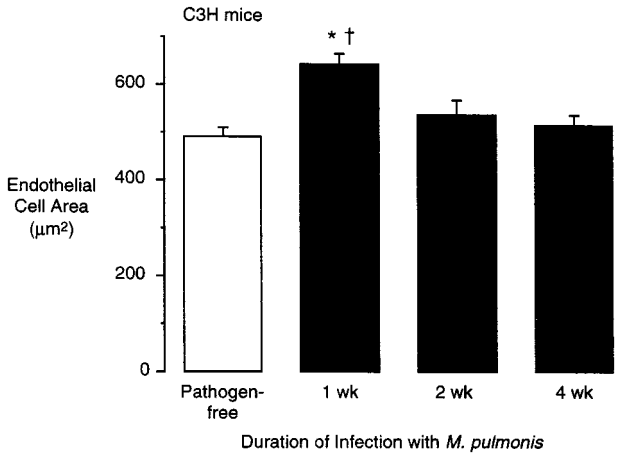

Figure 7. Luminal endothelial cell surface area in tracheal mucosa of pathogen-free and *M. pulmonis*-infected C3H mice. Endothelial cell area was measured in silver-nitrate-stained vessels in tracheal whole mounts by tracing cell borders on video microscopic projections with a digitizing tablet. Values represent mean ± SE of 10 venular endothelial cells per trachea and four tracheas per group ($n = 4$). *Significantly different from pathogen-free value; †significantly different from 4-week-infected value.

Plasma Leakage in Remodeled Vessels

The amount of Evans blue leakage per milligram of trachea in C3H or C57BL/6 mice infected for 4 weeks was similar to that in pathogen-free controls (Figure 9, A and B). However, substance P (5 μg/kg intravenously) caused significantly more leakage in infected mice of both strains than in pathogen-free controls (Figure 9, A and B). Thus, the remodeled vessels in *M. pulmonis*-infected mice of both strains were abnormally leaky in response to substance P.

Discussion

In this study we characterized the vascular remodeling associated with chronic inflammation induced by *M. pulmonis* infection in the airways of mice. By selectively staining the vasculature with lectins and examining the vessels in tracheal whole mounts, we found that the vascular remodeling was qualitatively different in two strains of mice. In C57BL/6 mice, the number of capillaries and venules doubled and the venules increased in size. In contrast, neither the length nor the number of vessels changed in C3H mice, but the size of the vessels doubled and the proportion of venules also doubled with a decrease in the proportion of capillaries and arterioles. The enlarged vessels in C3H mice contained more endothelial cells. Infected mice of both strains showed increased leakage in response to exogenous substance P but not increased baseline leakage. These findings show that the same chronic inflammatory stimulus in the airways can result in blood vessel proliferation and/or enlargement, depending on the genetically determined response of the host.

Time Course of Vascular Remodeling

In both C57BL/6 and C3H strains of mice, the vessel area density was increased at 1 week after infection and remained above baseline values at 2, 4, and 8 weeks. At 1 and 2 weeks, this increased vessel density reflected enlargement of the vessels. Some of this increased vessel size may be due to vasodilatation (ie, increased vessel diameter without increased numbers of endothelial cells), because the size of endothelial cells was increased at 1 week in C3H mice. This stage of the infection initiates production of several cytokines, including tumor necrosis factor-α, interleukin-1, and interleukin-6,[19] but precedes the appearance of significant titers of circulating antibodies to *M. pulmonis*.[18]

Subsequently, the number of vessels in the tracheal mucosa of infected C57BL/6 mice was increased in some focal regions at 4 weeks and was increased throughout the length of the trachea at 8 weeks. In comparison, the vessel diameters in C3H mice at 4 weeks and 8 weeks remained approximately twice their normal value, and no new vessel growth was detected. The size of the endothelial cells in tracheal vessels of C3H mice declined to control values at 2 and 4 weeks, despite unchanged vessel size, indicating increased numbers of endothelial cells. This process of remodeling appears to be an initial vasodilatation and endothelial cell enlargement, followed by an increase in the number of endothelial cells. The number of endothelial cells may have increased by proliferation of resident cells, although recruitment of circulating endothelial precursor cells to the vessel lumen may also occur.[28]

The initial stage of vascular remodeling (ie, vessel enlargement) was similar in the two strains, whereas new vessels grew only in C57BL/6 mice. The process of new vessel growth may be either a stage of vascular remodeling, driven by the severity or duration of the host inflammatory/immune response, or a distinct pathway, driven by a qualitatively different host response. By several criteria, C3H mice have a greater inflammatory/immune response to *M. pulmonis* infection,[18,19] yet no significant new vessel growth occurs. Thus, the new vessel growth in C57BL/6 mice and the vessel enlargement in C3H mice may not reflect differences in the severity of infection but instead may indicate qualitative differences in the inflammatory/immunological responses of the two strains. One scenario is that an innate immune response to *M. pulmonis* infection induces vessel dilatation, which, if prolonged for more than 1 to 2 weeks, can induce endothelial cell

Figure 6. Tracheal vasculature in pathogen-free and *M. pulmonis*-infected C3H and C57BL/6 mice. A: Smooth endothelial cell borders in tracheal venules of pathogen-free C3H mouse, stained by perfusion of silver nitrate. B: Irregular endothelial cell borders in silver-stained tracheal venules of C3H mouse infected for 4 weeks. Although borders are very irregular compared with pathogen-free mice, average luminal area of endothelial cells is similar. C: High-magnification view of trachea of C57BL/6 mouse infected for 8 weeks showing small capillary-like vessel (arrow) connected to venule (arrowhead). D: Example of blind vascular sprout (arrow) emanating from small vessel in trachea of C57BL/6 mouse infected for 4 weeks. E and F: Abrupt transitions from arterioles (arrows) to venule-like vessels (arrowheads) with little or no intervening capillary in tracheal vasculature of C3H mice infected for 4 weeks and stained with *L. esculentum* lectin (E) or silver nitrate (F). Adherent leukocytes in venules (double arrowheads). Scale bars, 20 μm (A and B), 20 μm (C), 10 μm (D), and 20 μm (E and F).

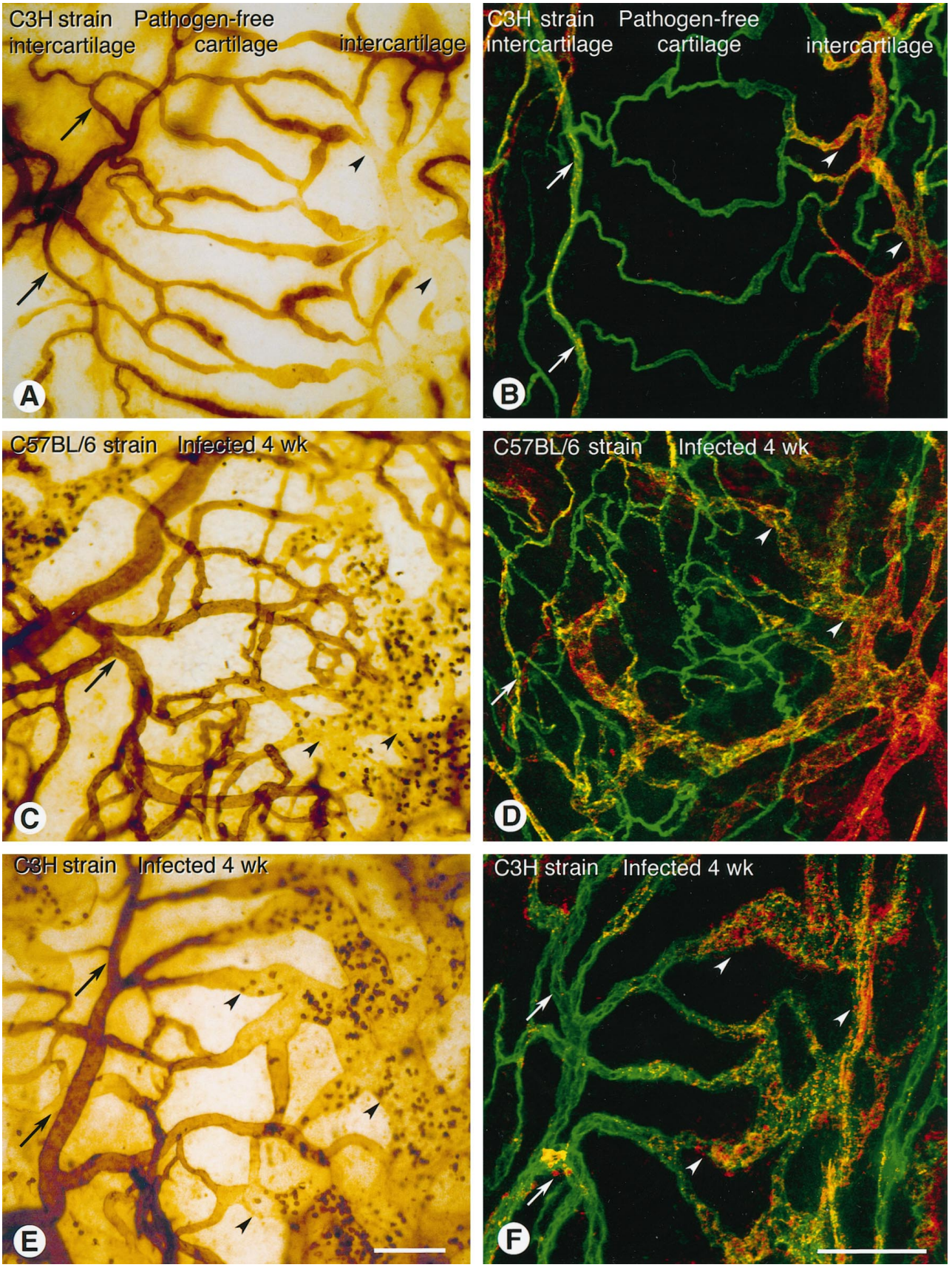
C3H strain Pathogen-free
intercartilage cartilage intercartilage
A
C3H strain Pathogen-free
intercartilage cartilage intercartilage
B
C57BL/6 strain Infected 4 wk
C
C57BL/6 strain Infected 4 wk
D
C3H strain Infected 4 wk
E
C3H strain Infected 4 wk
F

Table 1. Vessel Length Density and Relative Abundance in Tracheal Mucosa of Pathogen-Free and *M. pulmonis*-Infected C57BL/6 and C3H Mice

	Arterioles		Capillaries		Venules	
	Length density (mm/mm^2)	Fraction of total (%)	Length density (mm/mm^2)	Fraction of total (%)	Length density (mm/mm^2)	Fraction of total (%)
C57BL/6						
Pathogen-free	4.0 ± 0.3	17 ± 2	15.7 ± 1.0	65 ± 3	4.3 ± 0.5	18 ± 2
Infected 8 weeks	4.1 ± 0.3	9 ± 1*	27.3 ± 1.6*	63 ± 1	11.9 ± 0.8*	28 ± 1*
C3H						
Pathogen-free	4.2 ± 0.2	17 ± 2	14.3 ± 1.6	57 ± 3	6.4 ± 0.3	26 ± 2
Infected 8 weeks	2.8 ± 0.5*	14 ± 2	6.5 ± 1.1*	31 ± 5*	11.5 ± 1.3*	55 ± 6*

Vessel lengths were measured by tracing each type of vessel on video micrographs of *L. esculentum* lectin-stained tracheas with a digitizing tablet. The microscope field area for each set of vessel measurements was also determined (approximately 360 × 580 μm for each field). The fractional length of each vessel segment was determined by dividing the length density of that segment by the total length density and expressed as a percentage. Values are mean ± SE of four microscope fields per trachea and four tracheas per group ($n = 4$).

*Significantly different from corresponding pathogen-free values ($P < 0.05$, unpaired *t*-test).

proliferation but not new vessel growth. Subsequently, an acquired immune response can induce new vessel growth depending on the nature of that response. Further characterization of the inflammatory/immune responses in the two strains is needed to examine this question.

Angiogenesis in Chronic Inflammation

A potential source of confusion in describing changes in the microvasculature in chronic inflammation is usage of the term angiogenesis. Although often defined as the growth of new vessels from existing ones,[1,29,30] angiogenesis has also been used to describe vascular changes in chronic inflammation that involve endothelial cell proliferation without new vessel growth.[31,32] New vessel growth is readily identified in avascular tissues or in rapidly growing tissues such as tumors, but it may be difficult to identify in well vascularized tissues such as the airway mucosa. In the present study, we identified new vessel growth in the airways of chronically inflamed C57BL/6 mice that clearly corresponds to the usual definition of angiogenesis. However, in C3H mice, we identified vessel enlargement with increased numbers of endothelial cells but without new vessel growth. Should this type of microvascular remodeling also be considered as a form of angiogenesis? How prevalent is it in chronic inflammation? Refinement of the terminology used to describe these different microvascular responses would facilitate the communication of studies of chronic inflammation.

Endothelial Cell Phenotype

Endothelial cells in different segments of the microvasculature have specialized phenotypes.[22,24,33,34] For example, endothelial cells in venules are distinct from those in capillaries by virtue of their expression of receptors for certain inflammatory mediators,[35] lack of cell surface binding of the lectin WGA,[21] and adhesion of leukocytes and decreased barrier function after inflammatory stimuli.[16,27,34] It is unclear how these specialized phenotypic properties are regulated under normal or pathological conditions.

Although the biochemical basis and functional significance of the differential binding of WGA to the surface of endothelial cells is not known, it can be used as a phenotypic marker to help distinguish venules from capillaries. In the present study, we found that remodeled vessels in chronic inflammation in the two strains of mice differentially regulated this phenotypic marker. The luminal endothelial surface of new capillary-sized vessels in *M. pulmonis*-infected C57BL/6 mice bound WGA, indicating a similarity to capillaries. In contrast, the luminal endothelial surface of enlarged vessels in the location of capillaries in C3H mice did not bind WGA, indicating their conversion to a venule-like phenotype.

An additional feature that appears to distinguish different segments of the microvasculature is the amount of vWF immunoreactivity. Although vWF has been used as a marker for endothelial cells in culture and in tissue sections for many years, [22,24–26,36,37] most studies have

Figure 8. WGA-stained and vWF-immunoreactive vessels in tracheal whole mounts of pathogen-free and *M. pulmonis*-infected C57BL/6 and C3H mice. Biotinylated WGA was perfused and stained with ABC/DAB peroxidase reaction (A, C, and E). vWF was stained immunofluorescently using polyclonal primary antibody and Cy3-labeled secondary antibody (red/orange) on tracheas after the vessels were labeled by perfusion of fluorescein *L. esculentum* lectin (green; B, D, and F). vWF was imaged by confocal microscopy. A: Pathogen-free C3H mouse. WGA lectin binds strongly to arterioles (arrows) and capillaries across cartilaginous ring but weakly or not at all to venules (arrowheads). B: Pathogen-free C3H mouse, showing weak vWF immunoreactivity (red/orange) of capillaries across cartilaginous ring, strong immunoreactivity of venules (arrowheads), and moderate immunoreactivity of arterioles (arrows). C: C57BL/6 mouse infected for 4 weeks. WGA binds to arterioles (arrow) and the numerous small vessels across the cartilaginous ring, with little or no binding in enlarged vessels (arrowheads). Adherent leukocytes in venules show strong staining. D: C57BL/6 mouse infected for 8 weeks, showing moderate vWF immunoreactivity in arterioles (arrow), weak vWF immunoreactivity in the numerous small vessels across the cartilaginous ring, and strong immunoreactivity in enlarged venules (arrowhead). E: C3H mouse infected for 4 weeks. WGA binds strongly to endothelium in arterioles (arrows) but binds weakly or not at all to enlarged venules across the cartilaginous ring and in intercartilaginous regions (arrowheads). Adherent leukocytes in venules bind strongly. F: C3H mouse infected for 4 weeks, showing strong vWF immunoreactivity of the enlarged venules across the cartilaginous ring and in intercartilaginous regions (arrowheads) and much less in arterioles (arrows). Scale bars, 100 μm.

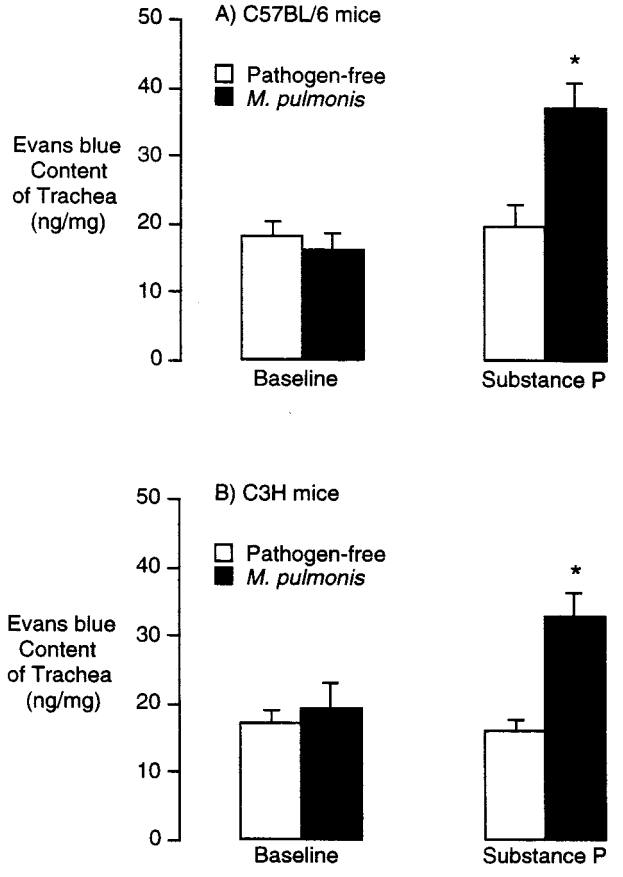

Figure 9. Evans blue leakage from tracheal vessels in pathogen-free and *M. pulmonis*-infected C57BL/6 and C3H mice. Evans blue was injected 5 minutes before injection of substance P (5 μg/kg) or vehicle, and the animals were perfused 5 minutes later. Evans blue was extracted from trachea and measured spectrophotometrically. Values represent the mean ± SE of six tracheas per group (n = 6). *Significantly different from corresponding pathogen-free values.

focused on endothelial cells from large vessels. The amount of vWF immunoreactivity is high in endothelial cells on the venous side of the circulation[22,25] and at sites of arterial branching[37] but low in capillaries.[24] However, the differential expression of vWF in different segments of the microvasculature has not been fully documented. In the present study, examination of the intact microvascular network in whole mounts of normal tracheas readily revealed that vWF immunoreactivity was moderate in arterioles, low in capillaries, and high in venules. Again, we found that remodeled vessels in chronic inflammation differentially regulated the amount of vWF. Endothelial cells of new capillary-sized vessels in *M. pulmonis*-infected C57BL/6 mice had very little vWF immunoreactivity, indicating their similarity to capillary endothelial cells, whereas endothelial cells of enlarged vessels in the location of capillaries in C3H mice had much more, indicating their conversion to a venule-like phenotype.

Adherent leukocytes were a prominent feature of chronically inflamed tracheas, particularly in C3H mice. Adherent leukocytes were not found in the new capillary-like vessels in infected C57BL/6 mice but were found in the enlarged venule-like vessels in C3H mice. Although some studies of chronically inflamed tissues have documented conversion of venules to lymph-node-like high endothelial venules specialized for lymphocyte migration,[38] the enlarged venules in tracheas of C3H mice infected with *M. pulmonis* did not show markers of high endothelial venules.[39]

Thus, in addition to the size, shape, and location of the vessels, we were able to use three phenotypic markers to assess whether endothelial cells had features of venules, namely, lack of binding of WGA, strong vWF immunoreactivity, and the ability to support adhesion of leukocytes. These markers were part of the phenotype of endothelial cells in normal venules and changed in a coordinated fashion in the remodeled vessels in chronically inflamed tracheas. vWF immunoreactivity was not strictly correlated with leukocyte adhesion or lack of WGA binding, as arterioles contained moderate amounts of vWF but bound WGA and did not support leukocyte adhesion. Therefore, this set of features appears to represent at least two independent markers of vessel phenotype. Examining changes in endothelial cell phenotype during vascular remodeling, and comparing the changes in the two types of remodeling in C57BL/6 and C3H mice, may help shed light on the regulation of specialized endothelial cell phenotype.

Although we have described the changes in endothelial cell phenotype in terms of features that can normally be used to distinguish capillaries from venules, additional phenotypic features may be distinctive to endothelial cells in remodeling or angiogenic vessels, and not found in the normal microvasculature. Some such features have recently been reported. For example, the integrin $\alpha_v\beta_3$[40] and the tie-family of tyrosine kinase receptors[41] may be selectively expressed by angiogenic endothelial cells. The relation between these distinctly angiogenic markers and the expression of capillary-like or venule-like phenotypes is unknown.

Plasma Leakage in Chronically Inflamed Tracheas

Previous studies have provided evidence for increased leakage of plasma from angiogenic blood vessels.[42] However, in the present study, we found that the baseline amount of plasma leakage was similar in pathogen-free mice and mice infected for 4 weeks, consistent with previous findings in F344 rats.[17] The method we used for assessing leakage, namely, measuring extravasated Evans blue dye in the whole trachea after a 5-minute circulation period, may not detect very localized leakage or brief episodes of leakage. Another possibility is that plasma leakage occurs earlier than 4 weeks and then ceases. Nevertheless, our findings indicate that despite the extensive vascular remodeling at 4 weeks, which is a period of rapid vessel growth in C57BL/6 mice, there is limited leakage under baseline conditions.

Unlike the baseline level of plasma leakage, the amount of leakage induced by substance P was much higher in infected mice than in pathogen-free mice. In rats, the abnormal sensitivity to substance P after *M. pulmonis* infection appears to be due, at least in part, to

up-regulation of receptors for substance P.[15] The role of the increased expression of substance P receptors in the pathophysiology of *M. pulmonis* infection is unknown, but the recent production of mice deficient in these receptors[43] may help answer the question.

Characterization of Vascular Remodeling in Tissue Whole Mounts

The different patterns of vascular architecture in infected C57BL/6 and C3H mice could be readily distinguished in lectin-stained tracheal whole mounts. In addition, as the location of individual vessels within the microvasculature could be identified, abnormalities in endothelial cell phenotype were also apparent. These features were not readily apparent in tracheas cut into thin sections. Although the whole-mount approach is not feasible with most pathological specimens, our findings indicate that different forms of vascular remodeling could be distinguished by morphometry of tissue sections combined with staining for specific markers of endothelial cell phenotype. For example, vascular remodeling similar to that observed in C3H mice could be detected in tissue sections by an increase in the diameter of the vessels without an increase in vessel number and by an increase in the proportion of vessels with strong vWF immunoreactivity.

Comparison with Other Studies of Vascular Remodeling in Chronic Inflammation

Although vascular remodeling is a common feature of chronic inflammation, few studies have documented the type of remodeling or the phenotype of endothelial cells in the remodeled vessels. Our previous studies of *M. pulmonis* infection of the airways of rats indicate that new capillary-sized vessels form in the tracheal mucosa of some strains of rat.[15] In infected F344 rats, new capillary-sized vessels form across the cartilage,[15] similar to the new vessel growth in C57BL/6 mice, but enlargement and proliferation of venules was not assessed in rats. Although different strains of rat also show different susceptibilities to *M. pulmonis*, we have not seen a vascular response similar to that of infected C3H mice in the strains that we have examined to date.

The type of vascular remodeling seen in C3H mice has been previously described in a model of aseptic chronic inflammation in adult rats.[32] In this model, a piece of sterile tissue was implanted next to the cremaster muscle, and the muscle capillaries enlarged and changed functional properties without the growth of new vessels. An increase in endothelial cell number was also reported, which was postulated to be a result of chronic hyperemia.[44]

Psoriasis is a chronic inflammatory condition in which the microvessels enlarge, become more tortuous, change their structural properties,[11–14] and contain proliferating endothelial cells.[11] The growth of new vessels via sprouting has not been documented in psoriasis. Dermal microvessels in the position of capillaries assume phenotypic properties of venules, as assessed by the ultrastructure of the basement membrane and the presence of endothelial fenestrae.[12] These particular phenotypic properties, which are visible only by transmission electron microscopy, may be specific to venules of the dermis, whereas other properties, such as the lack of binding of WGA lectin and high vWF immunoreactivity, have not been examined. Recently developed animal models of psoriasis[45] may help to characterize further the type of microvascular remodeling.

Morphometric studies of tissue sections from airway biopsies suggest that both the number and the size of vessels can increase in human asthma.[6,7,46] Characterization of the phenotypic properties of the vessels may further aid in defining the nature of the microvascular remodeling and in determining the amounts of new vessel growth and vessel enlargement in chronic airway inflammation.

Conclusions

We conclude that the vascular remodeling associated with *M. pulmonis* infection in mouse airways can include vessel proliferation and/or enlargement. Vessel proliferation results in new capillary- and venule-like vessels, whereas vessel enlargement results in the conversion of existing capillaries into venule-like vessels without new vessel growth. The differences in the remodeled vasculature reflect differences in the host response to the inflammatory stimulus and may play a role in the pathophysiology of the affected tissue.

Acknowledgments

We gratefully acknowledge Ms. Julie Erwin (University of Alabama) for providing the *M. pulmonis* organisms and for advice on infecting mice.

References

1. Risau W: Mechanisms of angiogenesis. Nature 1997, 386:671–674
2. Folkman J, Brem H: Angiogenesis and inflammation. Inflammation: Basic Principles and Clinical Correlates, ed 2. Edited by Gallin JI, Goldstein IM, Snyderman R. New York, Raven Press, 1992, pp 821–839
3. Colville-Nash PR, Scott DL: Angiogenesis and rheumatoid arthritis: pathogenic and therapeutic implications. Ann Rheum Dis 1992, 51: 919–925
4. Jackson JR, Seed MP, Kircher CH, Willoughby DA, Winkler JD: The co-dependence of angiogenesis and chronic inflammation. FASEB J 1997, 11:457–465
5. Dunnill MS: The pathology of asthma, with special references to changes in the bronchial mucosa. J Clin Pathol 1960, 13:27–33
6. Kuwano K, Bosken CH, Pare PD, Bai TR, Wiggs BR, Hogg JC: Small airways dimensions in asthma and in chronic obstructive pulmonary disease. Am Rev Respir Dis 1993, 148:1220–1225
7. Li X, Wilson JW: Increased vascularity of the bronchial mucosa in mild asthma. Am J Respir Crit Care Med 1997, 156:229–233
8. Telner P, Fekete Z: The capillary responses in psoriatic skin. J Invest Dermatol 1961, 36:225–230
9. Creamer JD, Barker JN: Vascular proliferation and angiogenic factors in psoriasis. Clin Exp Dermatol 1995, 20:6–9
10. Creamer JD, Allen M, Sousa A, Poston R, Barker JN: Altered vascular

endothelium integrin expression in psoriasis. Am J Pathol 1995, 147: 1661–1667
11. Braverman IM, Sibley J: Role of the microcirculation in the treatment and pathogenesis of psoriasis. J Invest Dermatol 1982, 78:12–17
12. Braverman IM, Yen A: Ultrastructure of the capillary loops in the dermal papillae of psoriasis. J Invest Dermatol 1977, 68:53–60
13. Barton SP, Abdullah MS, Marks R: Quantification of microvascular changes in the skin in patients with psoriasis. Br J Dermatol 1992, 126:569–574
14. Bacharach-Buhles M, Panz B, el Gammal S, Auer T, Altmeyer P: The elongation of psoriatic capillaries, the result of epidermal hyperplasia, not angiogenesis. J Invest Dermatol 1994, 103:263, A229
15. Baluk P, Bowden JJ, Lefevre PM, McDonald DM: Upregulation of substance P receptors in angiogenesis associated with chronic airway inflammation in rats. Am J Physiol 1997, 273:L565–L571
16. McDonald DM: Endothelial gaps and permeability of venules in rat tracheas exposed to inflammatory stimuli. Am J Physiol 1994, 266: L61–L83
17. McDonald DM, Schoeb TR, Lindsey JR: *Mycoplasma pulmonis* infections cause long-lasting potentiation of neurogenic inflammation in the respiratory tract of the rat. J Clin Invest 1991, 87:787–799
18. Cartner SC, Simecka JW, Lindsey JR, Cassell GH, Davis JK: Chronic respiratory mycoplasmosis in C3H/HeN and C57BL/6N mice: lesion severity and antibody response. Infect Immun 1995, 63:4138–4142
19. Faulkner CB, Simecka JW, Davidson MK, Davis JK, Schoeb TR, Lindsey JR, Everson MP: Gene expression and production of tumor necrosis factor α, interleukin 1, interleukin 6, and γ interferon in C3H/HeN and C57BL/6N mice in acute *Mycoplasma pulmonis* disease. Infect Immun 1995, 63:4084–4090
20. Faulkner CB, Davidson MK, Davis JK, Schoeb TR, Simecka JW, Lindsey JR: Acute *Mycoplasma pulmonis* infection associated with coagulopathy in C3H/HeN mice. Lab Anim Sci 1995, 45:368–372
21. Thurston G, Baluk P, Hirata A, McDonald DM: Permeability-related changes revealed at endothelial cell borders in inflamed venules by lectin binding. Am J Physiol 1996, 271:H2547–H2562
22. Aird WC, Edelberg JM, Weiler-Guettler H, Simmons WW, Smith TW, Rosenberg RD: Vascular bed-specific expression of an endothelial cell gene is programmed by the tissue microenvironment. J Cell Biol 1997, 138:1117–1124
23. Baluk P, Hirata A, Thurston G, Fujiwara T, Neal CR, Micheal CC, McDonald DM: Endothelial gaps: time course of formation and closure in inflamed venules of rats. Am J Physiol 1997, 272:L155–L170
24. Page C, Rose M, Yacoub M, Pigott R: Antigenic heterogeneity of vascular endothelium. Am J Pathol 1992, 141:673–683
25. Rand JH, Badimon L, Gordon RE, Uson RR, Fuster V: Distribution of von Willebrand factor in porcine intima varies with blood vessel type and location. Arteriosclerosis 1987, 7:287–291
26. Wu QY, Drouet L, Carrier JL, Rothschild C, Berard M, Rouault C, Caen JP, Meyer D: Differential distribution of von Willebrand factor in endothelial cells: comparison between normal pigs and pigs with von Willebrand disease. Arteriosclerosis 1987, 7:47–54
27. Umeno E, Nadel JA, McDonald DM: Neurogenic inflammation of the rat trachea: fate of neutrophils that adhere to venules. J Appl Physiol 1990, 69:2131–2136
28. Asahara T, Murohara T, Sullivan A, Silver M, vanderZee R, Li T, Witzenbichler B, Schatteman G, Isner JM: Isolation of putative progenitor endothelial cells for angiogenesis. Science 1997, 275:964–967
29. Folkman J, Shing Y: Angiogenesis. J Biol Chem 1992, 267:10931–10934
30. Hanahan D, Folkman J: Patterns and emerging mechanisms of the angiogenic switch during tumorigenesis. Cell 1996, 86:353–364
31. Wolf JEJ: Angiogenesis in normal and psoriatic skin. J Clin Invest 1989, 61:139–142
32. Joris I, Cuenoud HF, Underwood JM, Majno G: Capillary remodeling in acute inflammation: a form of angiogenesis. FASEB J 1992, 6:A938
33. Gerritsen ME: Functional heterogeneity of vascular endothelial cells. Biochem Pharmacol 1987, 36:2701–2711
34. Majno G, Palade GE, Schoefl GI: Studies on inflammation. II. The site of action of histamine and serotonin along the vascular tree: a topographic study. J Biophys Biochem Cytol 1961, 11:607–625
35. Bowden JJ, Garland AM, Baluk P, Lefevre P, Grady EF, Vigna SR, Bunnett NW, McDonald DM: Direct observation of substance P-induced internalization of neurokinin 1 (NK1) receptors at sites of inflammation. Proc Natl Acad Sci USA 1994, 91:8964–8968
36. Weidner N: Current pathologic methods for measuring intratumoral microvessel density within breast carcinoma and other solid tumors. Breast Cancer Res Treat 1995, 36:169–180
37. Senis YA, Richardson M, Tinlin S, Maurice DH, Giles AR: Changes in the pattern of distribution of von Willebrand factor in rat aortic endothelial cells following thrombin generation in vivo. Br J Haematol 1996, 93:195–203
38. Zoellner HF, Hunter N: High endothelial-like venules in chronically inflamed periodontal tissues exchange polymorphs. J Pathol 1989, 159:301–310
39. Thurston G, Murphy TJ, Erwin J, Lindsey JR, McDonald DM: Changes in endothelial cell phenotype in chronic inflammation of mouse airways. Am J Crit Care Respir Med 1997, 155:A124
40. Brooks PC, Clark RA, Cheresh DA: Requirement of vascular integrin $\alpha v\beta 3$ for angiogenesis. Science 1994, 264:569–571
41. Korhonen J, Partanen J, Armstrong E, Vaahtokari A, Elenius K, Jalkanen M, Alitalo K: Enhanced expression of the tie receptor tyrosine kinase in endothelial cells during neovascularization. Blood 1992, 80:2548–2555
42. Dvorak HF, Brown LF, Detmar M, Dvorak AM: Vascular permeability factor/vascular endothelial growth factor, microvascular hyperpermeability, and angiogenesis. Am J Pathol 1995, 146:1029–1039
43. Bozic CR, Lu B, Hopken UE, Gerard C, Gerard NP: Neurogenic amplification of immune complex inflammation. Science 1996, 273: 1722–1725
44. Majno G, Joris I: Cells, Tissue, and Disease. Cambridge, MA, Blackwell Science, 1996, p 379
45. Schon MP, Detmar M, Parker CM: Murine psoriasis-like disorder induced by naive $CD4^+$ T cells. Nature Med 1997, 3:183–188
46. Charan NB, Baile EM, Pare PD: Bronchial vascular congestion and angiogenesis. Eur Respir J 1997, 10:1173–1180